Spatiotemporal shoreline dynamics of Namibian coastal lagoons derived by a dense remote sensing time series approach

Robert Behling*, **Robert Milewski, Sabine Chabrillat**

Remote Sensing Section - GFZ German Research Centre for Geosciences, Telegrafenberg, 14473 Potsdam, Germany

* Corresponding author

E-mail: robert.behling@gfz-potsdam.de, robert.milewski@gfz-potsdam.de, sabine.chabrillat@gfz-potsdam.de

ABSTRACT

This paper proposes the remote sensing time series approach WLMO (Water-Land MOnitor) to monitor spatiotemporal shoreline changes. The approach uses a hierarchical classification system based on temporal MNDWI-trajectories with the goal to accommodate typical uncertainties in remote sensing shoreline extraction techniques such as existence of clouds and geometric mismatches between images. Applied to a dense Landsat time series between 1984 and 2014 for the two Namibian coastal lagoons at Walvis Bay and Sandwich Harbour the WLMO was able to identify detailed accretion and erosion progressions at the sand spits forming these lagoons. For both lagoons a northward expansion of the sand spits of up to 1000m was identified, which corresponds well with the prevailing northwards directed ocean current and wind processes that are responsible for the material transport along the shore. At Walvis Bay we could also show that in the 30 years of analysis the sand spit's width has decreased by more than a half from 750m in 1984 to 360m in 2014. This ongoing cross-shore erosion process is a severe risk for future sand spit breaching, which would expose parts of the lagoon and the city to the open ocean. One of the major advantages of WLMO is the opportunity to analyze detailed spatiotemporal shoreline changes. Thus, it could be shown that the observed long-term accretion and erosion processes underwent great variations over time and cannot a priori be assumed as linear processes. Such detailed spatiotemporal process patterns are a prerequisite to improve the understanding of the processes forming the Namibian shorelines. Moreover, the approach has also the potential to be used in other coastal areas, because the focus on MNDWI-trajectories allows the transfer to many multispectral satellite sensors (e.g. Sentinel-2, ASTER) available worldwide.

Keywords: coastal lagoons, spatiotemporal dynamics, remote sensing, time series, shoreline

1 INTRODUCTION

Globally, coastal areas are densely populated ecosystems of high ecological, economic, and social importance (Costanza et al., 1997; Martínez et al., 2007). Coastal lagoons in particular play an important role as productive ecosystems, species-rich habitats, and areas for storm protection and tourism (Anthony et al., 2009). Along Namibia's west coast, the lagoons are separated from the Atlantic Ocean by sand spits formed along the shore. Two prominent Namibian lagoons are Walvis Bay and Sandwich Harbour (Glassom and Branch, 1997; Lass and Mohrholz, 2005; Miller and Becker, 2008) (Fig. 1). The sand spits forming the two lagoons are highly dynamic and are known to have altered their shape in historical time (DMC and CSIR, 2010; Schoonees et al., 1998; e.g. Wilkinson et al., 1989). Aeolian processes and longshore or cross-shore drifts are the main causes of these sand spit variations (Hughes et al., 1992; Schoonees et

al., 1998). In the long run such processes can lead to a diminishing of the lagoons either by a sedimentation of the lagoons or by a breaching of the sand spits that exposes the lagoons to the open ocean (Schoonees et al., 1998). Since such changes endanger the important habitats as well as the shipping and the port at Walvis Bay, a detailed knowledge about the spatiotemporal variations in the sand spits is of high relevance. So far, only long-term changes are determined using historical maps and aerial photographs of several years or decades apart (Elfrink et al., 2003; Schoonees et al., 1998; Wilkinson et al., 1989), and single point-based measurement for a short period of month are conducted (Lass and Mohrholz, 2005). However, to enable the analysis of the relationship between forcing processes and actual sediment transports requires frequent assessments of the sand spits shoreline variations over longer periods.

Traditional ground-survey techniques for shoreline extraction (Natesan et al., 2013) and techniques using airborne (i.e. platforms on planes and UAVs) data acquisitions of optical photographs (Cermakova et al., 2016; Long et al., 2016), SAR-data (Bates et al., 2006), or LiDAR data (Stockdon et al., 2002) are accurate, but time-consuming, labor and cost intensive, and don't allow past assessments due to missing data. Detailed reconstruction of past shoreline variations requires the availability of frequent past image acquisitions with sufficient spatial resolution. Satellite remote sensing images of high spatial resolution (e.g. Quickbird, Worldview) used by Lee (2016) and Mann and Westphal (2014) are sufficient in spatial resolution but lack temporal data frequency. Landsat images are globally freely available at 30m spatial resolution with a 16 day repeat rate, which are considered as suitable for large scale shoreline changes at a fairly high frequency. Thus, Landsat imagery was frequently used to investigate developments of oceanic coasts in general (Ghosh et al., 2015; Li and Damen, 2010; Maiti and Bhattacharya, 2009; Wang et al., 2017) and to map shoreline variations at coastal lagoons to analyze erosion and accretion processes (e.g. Ahmed et al., 2009; El-Asmar and Hereher, 2011; Kuleli, 2010).
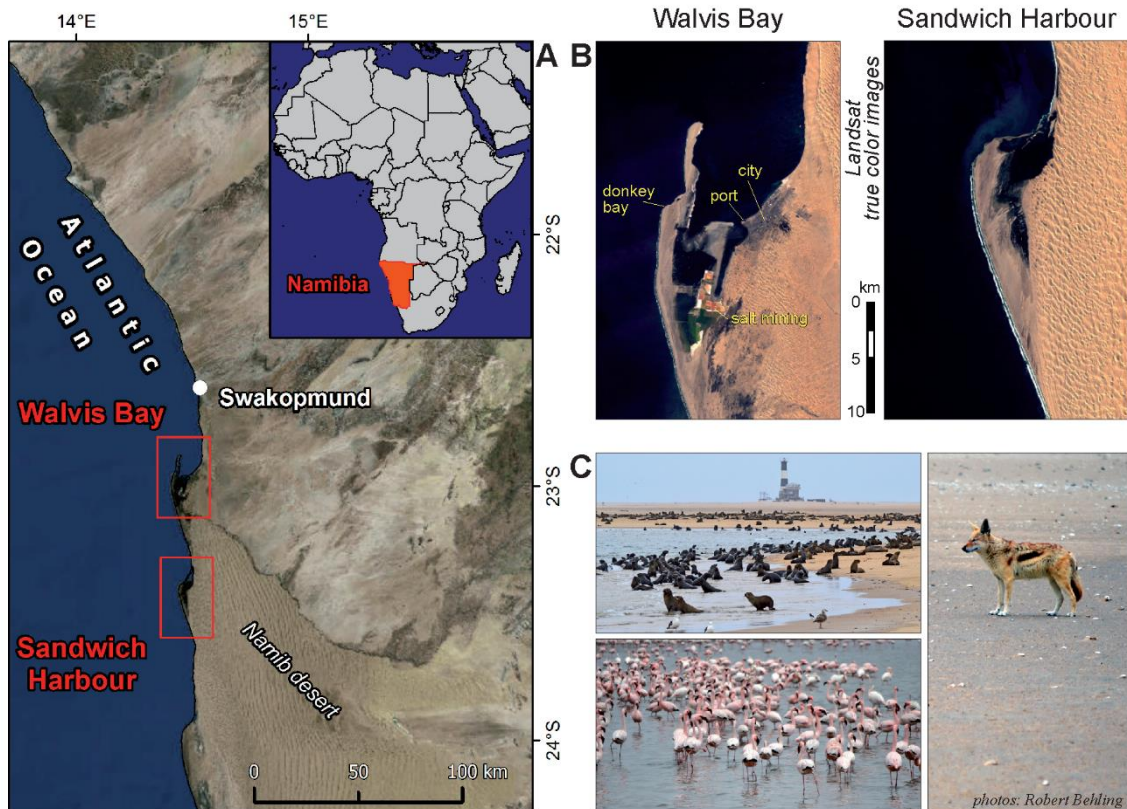
Regardless of the used satellite sensor, the assessment of shoreline changes is based on two major steps: (i) shoreline detection in each dataset and (ii) shoreline change estimation between subsequent images. The first step involves the binarization of images to distinguish between water and non-water pixels by techniques such as image thresholding, classification, and segmentation. The second step includes the change estimation along defined transects or the determination of overall changed areas based on the binarized images or shoreline vectors extracted from these binary results. For both steps an overview of techniques can be found in Aedla et al. (2015), Louati et al. (2015), and Wang et al. (2017). In general, the determination of overall change underlies uncertainties that get introduces during both steps. The ability and accuracy to extract the shoreline position in an image is influenced by the existence of clouds, turbidity, fog, tidal areas, wet surfaces, and mixed pixels at the water-land front (Ryu et al., 2002). Moreover, finding a threshold or classification rule that applies to all images of a time series is almost impossible. The actual change estimate, the second step, is further influenced by geometric mismatches or tidal variations between the compared images. All these uncertainties play a varying role in each image and if using a large number of images they can lead to a large overestimation of the overall change rate determination. In fact, the overall accuracy of such post-classification comparisons is generally considered to be intrinsically low (Coppin et al., 2004), which is probably the main reason why shoreline change studies so far used only few images of years or even decades apart even if more imagery would have been available.

80   In this paper we propose a shoreline change rate determination technique, which uses the high temporal
81   information content of a dense Landsat time series with the goal to reduce the influence of uncertainty
82   effects in remote sensing image shoreline change rate determination. Therefore, we use a time series
83   change detection approach analyzing variations in the temporal domain and neglecting the shoreline
84   position extraction for each image. This approach was named Water-Land MOnitor (WLMO) and applied
85   for two of the most important Namibian lagoons at Walvis Bay and Sandwich Harbour to analyze how
86   long-term (e.g. longshore drifts and main wind direction) and short-term processes (e.g. storm events)
87   shape the sand spits at these lagoons and to evaluate potential hazards endangering the lagoons existence.

88   **2 STUDY SITES AND DATA**

89   **2.1 Study Sites**

90   The study sites Walvis Bay and Sandwich Harbour are located at the western Namibian coast, south of
91   Swakopmund (Fig. 1). The sand spits forming the coastal lagoons are several kilometers long and hundreds
92   of meters wide. Both lagoons are part of the Ramsar convention, which is an international treaty for the
93   conservation and sustainable use of internationally important wetlands (Ramsar, 2016). The Benguela
94   current causes an upwelling of nutrient-rich deep ocean water, which results in a high biological
95   production (DMC and CSIR, 2010). They are important habitats for large bird populations (e.g. flamingos
96   and pelicans), fish populations (e.g. steenbras, kabeljou) and mammals (e.g. seals). The study sites are
97   extremely dry with an annual rainfall of less than 20mm and due to the cold ocean water the area is subject
98   to frequent formation of fog (Hughes et al., 1992; Roux, 1974; Schoonees et al., 1998). The sand spits present
99   sandy and erodible land without any vegetation (Hughes et al., 1992) (Fig. 1c). Tides are semi-diurnal with
100   a mean tide range of 1.42 m and 0.62 m for spring tides and neap tides, respectively (DMC and CSIR, 2010;
101   Hughes et al., 1992). The prevailing winds are strong southwesterlies (Hughes et al., 1992; Roux, 1974). The
102   dominant wave direction is from south to south-westerly with a median significant wave height of 1.1 m
103   (Elfrink et al., 2003; Hughes et al., 1992; Schoonees et al., 1998). The sand spit of Walvis Bay protects a
104   town with the main deep water port of Namibia and a salt mining company in the direct vicinity (DMC
105   and CSIR, 2010; Elfrink et al., 2003; Schoonees et al., 1998). Sandwich Harbour was anchorage for whalers
106   for many decades in the 19th century but since then no substantial development took place and today it is
107   mainly used for occasional touristic activities (Wilkinson et al., 1989).

Figure 1 Study sites: a) Location of the study sites, b) Landsat imagery showing the study sites of Walvis Bay and Sandwich Harbour. d) pictures of Walvis Bay mixed water-land landscape and rich fauna.

2.2 Data

The remote sensing database comprises Landsat images of the sensors TM, ETM+, and OLI covering 30 year period between 1984 and 2014. The images are retrieved from the USGS EarthExplorer (http://earthexplorer.usgs.gov/) as orthorectified Level 1T data. Both lagoons are located in the overlapping area between two Landsat WRS2 paths (path/row: 179/76 and 180/76), which allows for a higher temporal data repetition rate than usual. Images were selected on the basis that at least a part of a lagoon was cloud- and fog-free. In total, 130 images for Walvis Bay and 147 images for Sandwich Harbour were available (Fig. 2), representing an annual average of more than 4 images. At Sandwich Harbour data gaps exist in 1985, 1988, 2011, and 2012. At Walvis Bay, acquisitions in two more years (1987 and 1995) are missing. The selected images have varying coverage of clouds, fog, flooded tidal areas, white spume on waves, and milky water due to Sulphur eruptions (Supplements 1, 2), which all have the potential to hamper the discrimination between water and land.

123
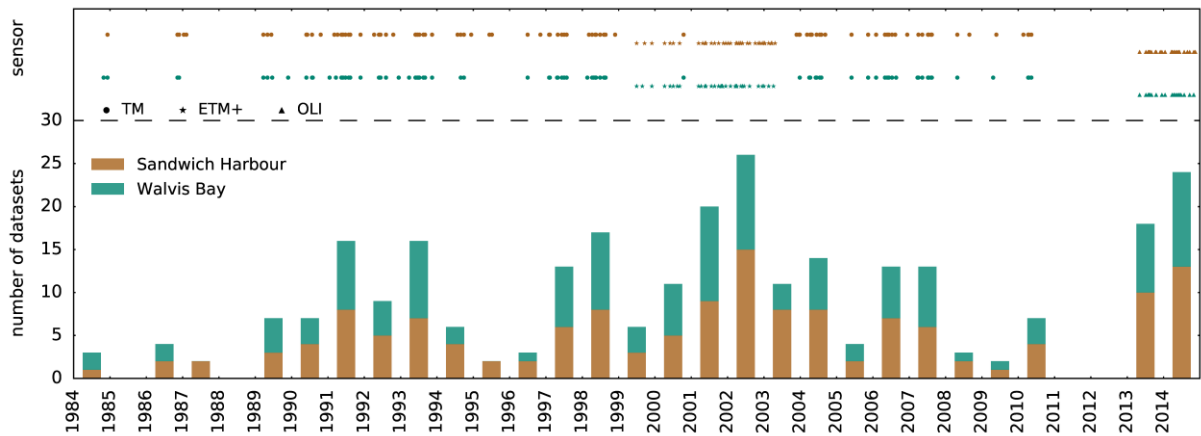
Figure 2 Database of partially cloud.- and fog-free Landsat images available at the study sites.

124

3 METHOD

125

126 The WLMO (Water-Land MOnitor) is based on the analysis of temporal trajectories of the Modified
127 Normalized Differenced Water Index (MNDWI) of Xu (2006). In the following the WLMO is described in
128 terms of performed remote sensing data pre-processing (Sec 3.1), the developed MNDWI trajectory
129 analysis method including its output parameters (Sec 3.2), and the validation procedure (Sec. 3.3)

3.1   Pre-processing

130

131 As a prerequisite for time series analysis the remote sensing images have to be comparable in their
132 information content (Coppin et al., 2004). To meet the homogenization requiremnt, the Landsat images
133 were converted from DN to Top of Atmosphere (TOA)-reflectance to adjust for radiometric scene
134 variations caused by solar illumination differences, sensor specific gains and offsets, and differences in
135 seasonality (Earth-Sun distance). Furthermore, relative image-to-image co-registration was performed to
136 minimze artifact changes due to spatial misalignements. Therfore, the co-registration approach of Behling
137 et al. (2014) was applied for each lagoon seperately resulting in sub-pixel image-to-image alignemnt.

3.2   Analysis of erosion and accretion processes using temporal MNDWI trajectories

138

139 For each Landsat image the MNDWI of Xu (2006) was calculated and stacked to a MNDWI temporal data
140 cube (Fig. 3). The MNDWI represents a ratio of the green and mid-infrared (MIR) spectral bands, utilizing
141 the extreme low infrared reflectance of liquid water to discriminate between water and land bodies.
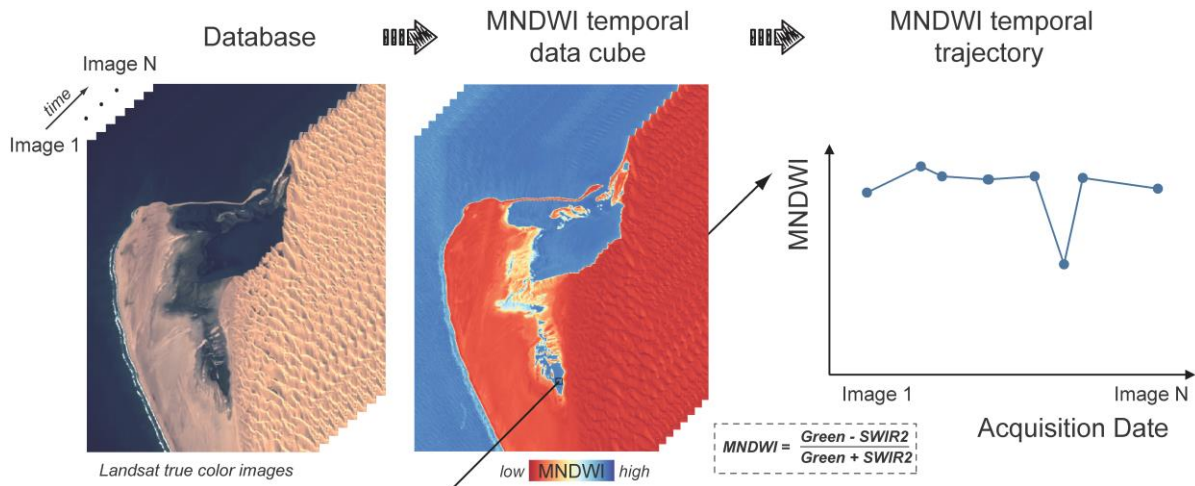
142

143

Each pixel of the MNDWI temporal data cube represents a temporal MNDWI trajectory (Fig. 3). Based on these temporal MNDWI trajectories the WLMO approach implements a hierarchical classification system (Fig. 4) for the detection of water-land transitions, which can be interpreted in terms of erosion and accretion processes. At top level, temporally stable and unstable areas are distinguished. The stable areas are subdivided into permanent water and permanent land. The unstable areas into single erosion, single accretion, or multiple land/water transitions.
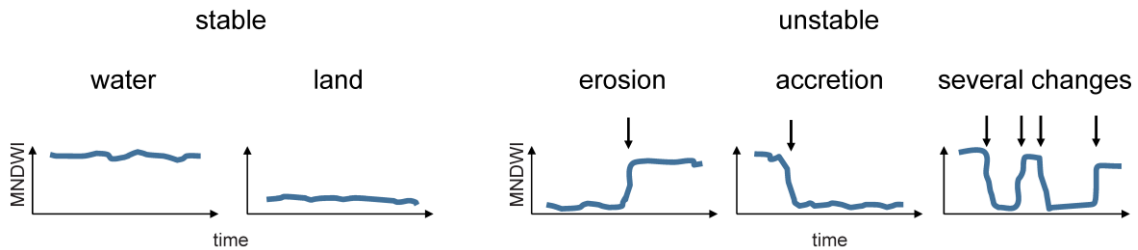
150

151
152

The MNDWI trajectory-based classification of WLMO comprises four processing steps (Fig. 5). Step A: Smoothing of the MNDWI-trajectories using a temporal median filter (kernel size = 3) (Fig. 5a). This filtering removes outliers caused by cloud coverage, fog/haze, or temporally flooding. On the other hand it preserves longer-term variations such as erosion and accretion processes. Step B: Classification into sure pixels (water/land) and unsure pixels (mixture of both). Pixels are classified into sure open water (MNDWI>0.6) and sure land pixels (MNDWI<0.0) based on the median filtered MNDWI-trajectory (Fig. 5b). The remaining non-classified pixels are interpreted as a mixed signal of water and land due to influences of haze, fog, moist surfaces, or sub-pixel mixtures at the shoreline between water and land. Thus, they either represent pixels with a disturbed signal or pixels during transition periods from land to water (erosion: t_e) or water to land (accretion: t_a). Step C: Gap filling between the sure pixels and identification of transition periods. The identification of transition periods relies on the temporal adjacent classes of sure water or sure land. If the sure classes match, the acquisitions in between are classified accordingly, and if not, a transition period is identified (Fig. 5c). Step D: Determination of the date of change during each transition period (Fig. 5d). The date of change during transition is associated with the period between subsequent images (pre- and post-image) of highest MNDWI change.
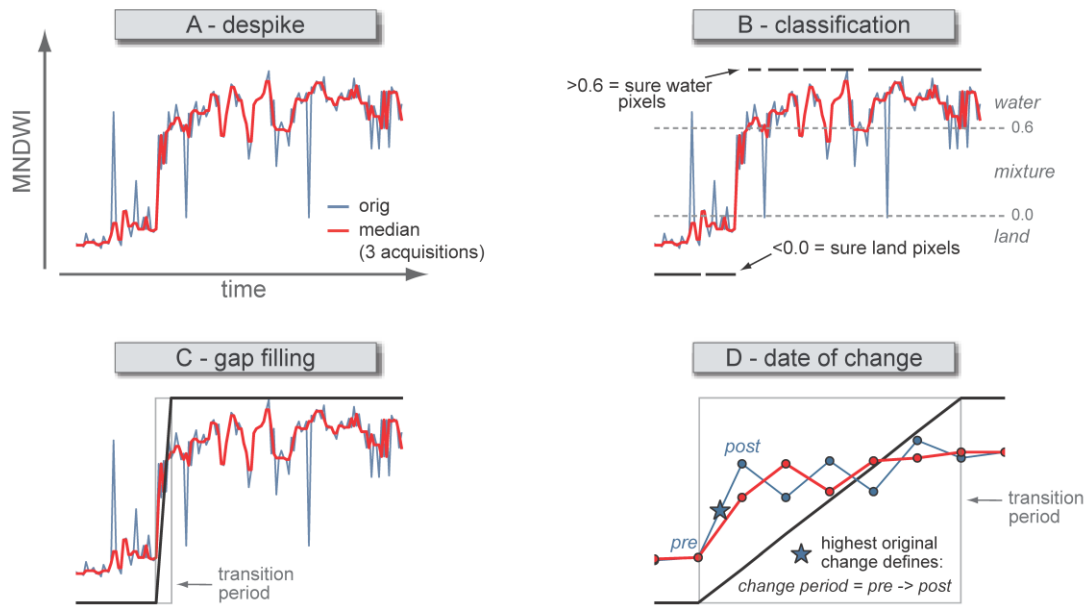
Figure 5 Processing steps for pixel-based MNDWI trajectory analysis in WLMO.

The result of the WLMO is a pixel-based binary temporal trajectory classifying each acquisition in water or land. Based on the binary trajectory the following parameters are provided:

- type of occurring transitions: erosion (t_e), accretion (t_a)
- date of transitions: period between subsequent images
- total number of transitions (t_{No}): $\Sigma t_{e/a}$
- overall stability:
  - stable pixels ($t_{No} == 0$). Further classified in permanent water or permanent land
  - unstable pixels ($t_{No} > 0$). Further characterized by change dominance: erosion ($\Sigma t_e > \Sigma t_a$), accretion ($\Sigma t_e < \Sigma t_a$), no dominance ($\Sigma t_e < \Sigma t_a$)

3.3 Validation procedure

Due to the lack of existing reference data for past spatiotemporal progression of accretion and erosion processes at Walvis Bay and Sandwich Harbour, a detailed quantitative accuracy assessment is not possible. Therefore, we evaluated the quality of the obtained results by comparing the results of the change detection analysis with visual assessments of randomly selected available Landsat acquisitions and with published knowledge in the area. Moreover, we assessed how tide variations influence shoreline positions and evaluated how they influence the shoreline change determination results of WLMO.

4 RESULTS

The WLMO approach was applied to the Landsat time series for Walvis Bay and Sandwich Harbour. This section shows the achieved results in increasing detail. Section 4.1 presents the general output parameters of WLMO that differentiate the stability and dominant change processes (i.e. erosion or accretion). Section 4.2 provides annual spatiotemporal change rates of erosion and accretion for sub-regions of major changes. Section 4.3 shows the temporal development of the shoreline along two transects to demonstrate the temporal details that is achieved. Section 4.4 evaluates the quality of the derived WLMO results.

4.1 Detection and mapping of erosion and accretion processes

Fig. 6 depicts the WLMO results for both study sites, discriminating stable areas into water and land and characterizing unstable areas by change dominance and number of transitions. Unstable areas with a low number of transitions represent distinct accretion or erosion processes, whereas many transitions indicate that these areas are very variable over time. Distinct erosion or accretion processes are prevalent at the western flank of the sand spits, which are exposed to the open ocean. At Walvis Bay the tip and the shoulder (i.e. donkey bay) of the western flank accreted and the north-western flank eroded over the analyzed 30-year period. At Sandwich Harbour the whole western flank and tip of the sand spit was steadily growing, whereas steady long-term erosion processes are not identified. Overall, both sand spits expanded in northern direction. with up to 950m at Walvis Bay and 1050m at Sandwich Harbour (Fig. 7).
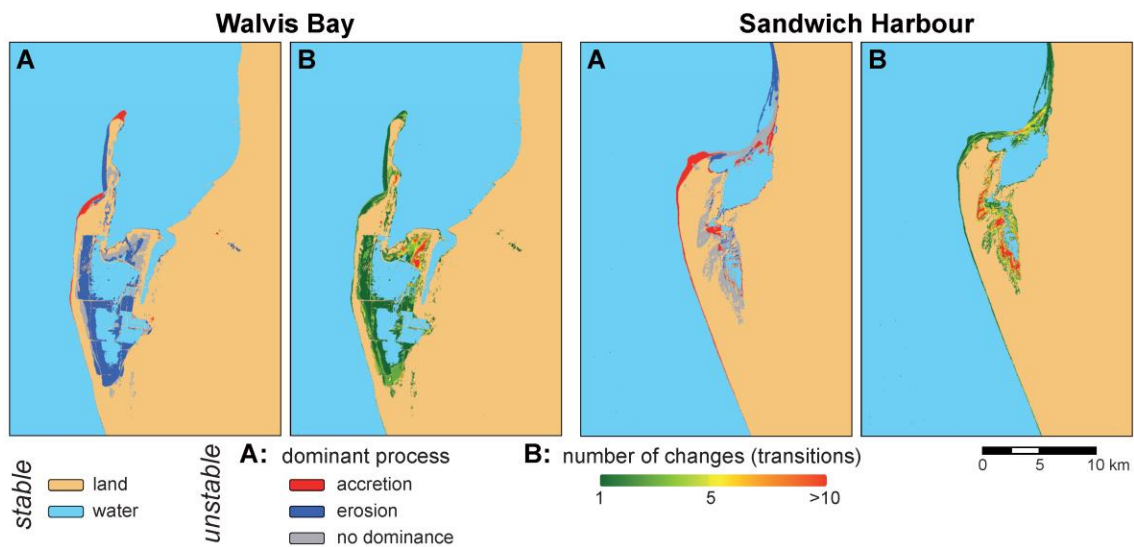
Figure 6 Results for both coastal lagoons in terms of temporal stability (stable vs. unstable). Temporal unstable pixels are differentiated in terms of a) overall dominant change process and b) number of overall water-land transitions.

207
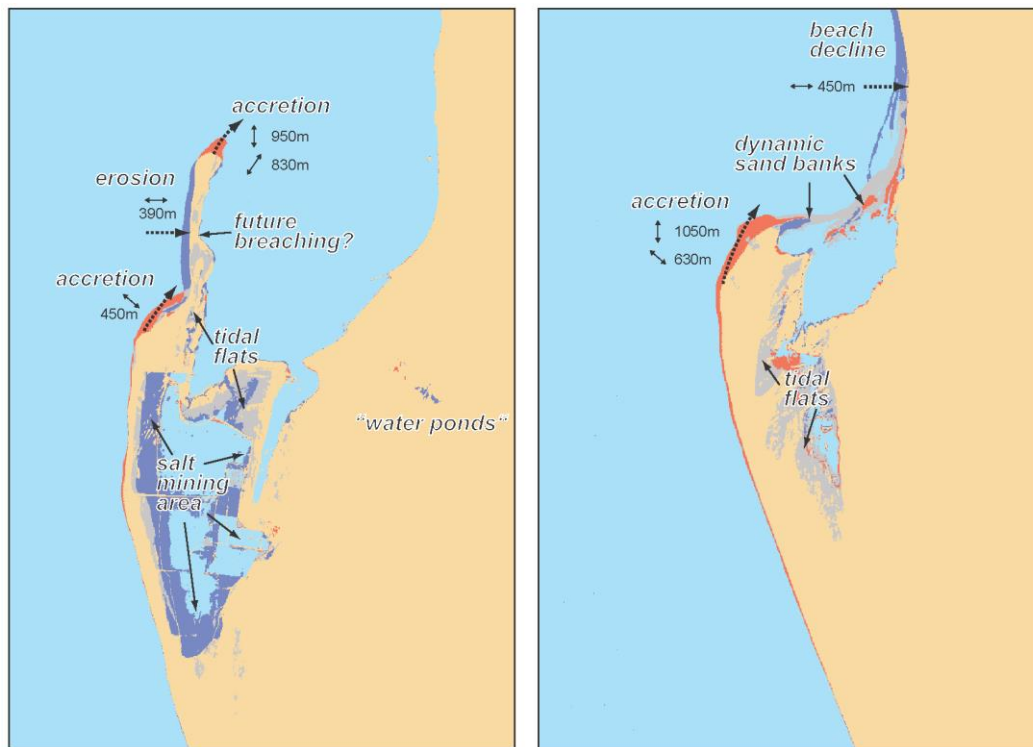
Figure 7 Interpretation of major change areas along with distances (number in meter) and directions (double headed arrows) of detected change. Left: Walvis Bay. Right: Sandwich Harbour (For color legend refer to Fig. 6A)

In contrast to the western flanks, the eastern flanks of the sand spits are rather stable. In case of Walvis Bay, at the northern end of the sand spit, the combination of eroding western flank and stable eastern flank results in a decreasing width of the sand spit. At the thinnest location the sand spit has reduced its width by 390m from 750m in 1984 to 360m in 2014 (Fig. 7). This substantial erosion by more than a half of the sand spit's width clearly reveals the risk of future breaching, which would expose the city and the port of Walvis Bay to the open ocean.

The regions that are protected by the sand spits experienced various change processes. The most obvious change is the large "eroding" area at Walvis Bay, which is caused by the expansion of the ponds of the salt mining company (DMC and CSIR, 2010). In contrast to these anthropogenic changes, further regions of frequent land/water transitions exist in both lagoons. These are naturally caused changes representing tidal flats, where the fluctuating tides cause temporary flooding and drying (Fig. 7).

At Sandwich Harbour two additional phenomena could be identified. Northeast of the main sand spit a variable development of small sand banks occurred. These sand banks grew from the sand spit in northeastern direction towards the mainland, but breached occasionally before they could totally cut off the lagoon from the open see water (Supplement 2). The second phenomenon is the beach decline from west to east at the main coast in the northern part of the studied subset (Fig. 6, 7).

4.2. Annual spatiotemporal change patterns for selected regions with dominant change regions

For a deeper insight in the dynamics of the observed processes we analyzed the obtained results regarding annual spatiotemporal change patterns (Fig. 8, 9). In general the derived change patterns reveal that the dominating erosion or accretion processes were not a linear process but were rather characterized by great variations over time. For example, the northeastern progression of the tip of the Walvis Bay sand spit (Fig.

8A3) has resulted in a total expansion of 0.39km² over the last 30 years (Fig. 8B3), which represents a long-term average accretion rate of 13,000m²/a. However, this overall steady accretion varied greatly and underlay strong phases of accretion (up to 103,500m²/a in 1989), but also phases of marginal accretion (e.g. 3600m²/a in 1994), and even years with dominant erosion (77,400m²/a in 1986) (Fig. 8B3). Another example is the erosion at the western flank of the Walvis Bay sand spit (Fig. 8 A1). In 30 years this eastern directed process eroded overall 1.86 km² of the western sand spit (Fig. 8 B1), which is almost five times the 0.39km² accretion at the tip. The long-term annual average of erosion is 62,000m² and the annual erosion rate peaks in 1999 with 268,200m² exceeding the long-term average by more than four times. The largest observed changes are caused by the expansion of sea water pre-evaporation ponds used for salt mining (Fig. 8 A2). In 1989, 2000, and 2001 annual "erosion rates" of more than 3km² could be observed due to these pond expansions.
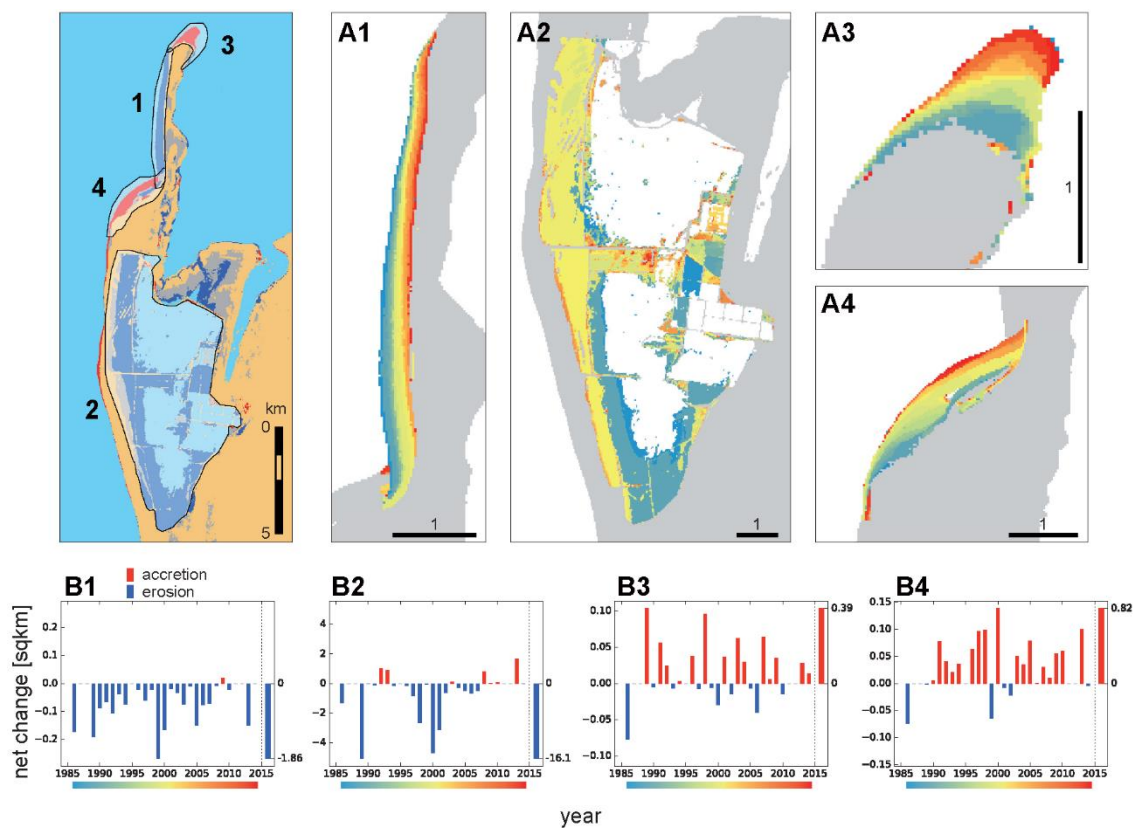
Figure 8 Spatiotemporal change patterns at Walvis Bay. a) Spatiotemporal progression of either erosion or accretion processes (color represents the year the pixel was first eroded/accreted), b) annual net change rate of erosion and accretion pixels (each pixel covers 900m²). Missing data in 1987, 1988, 1995, 2011, and 2012 (see Fig. 2). Four sub-regions are shown with either dominating erosion or accretion: 1 - Accretion at tip of sand spit, 2 - Erosion of the western flank, 3 - Accretion at donkey bay, 4 "Erosion" caused by salt mining.

At Sandwich Harbour the findings reveal that the "beach decline" at the northeastern part occurred in two separate periods (Fig. 9A2, 9B2). At first a strong erosion took place around 1990, followed by a more stable period of low erosion and even accretion phases. The tip of the Sandwich Harbour expanded constantly in northern direction by a total of 1.71km² over the 30 years (Fig. 9A1, 9B1), which is more than four times the expansion observed at the tip at Walvis Bay (0.39km²).
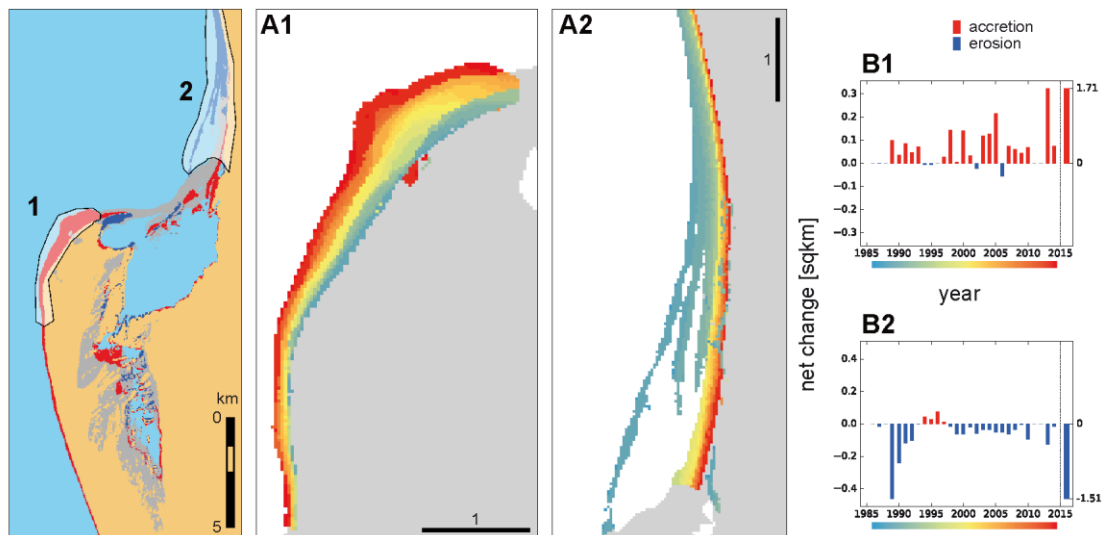
Figure 9 Spatiotemporal change patterns at Sandwich Harbour. a) Spatiotemporal progression of either erosion or accretion processes (color represents the year the pixel was first eroded/accreted), b) annual net change rate of erosion and accretion pixels (each pixel covers 900m²). Missing data in 1988, 2011, and 2012 (see Fig. 2). Two sub-regions are shown of either dominating erosion or accretion: 1 Accretion at tip of sand spit. 2: Erosion of beaches NE of sand spit.

4.3 Detailed erosion and accretion progression along transects

We analyzed the progression of erosion and accretion processes along transects (Fig. 10) in two selected areas of major change: (i) for the northern expansion of Sandwich Harbour and (ii) for the shrinkage of the western flank of the sand spit at Walvis Bay. This analysis allows to reveal detailed temporal variations of the longer-term progressing erosion and accretion processes. Along the transect at Walvis Bay (Fig. 10B) the sand spit has receded 420m during the 30 year period, representing a long-term average rate of 14m/a. Until 2007 the sand spit receded constantly with an annual rate of 16.6m followed by a stable period. This stability in recent years could also be observed for the complete southern part of the western flank, whereas the northern part has been subject to a higher erosion intensity during this period (Fig. 10B, left panel).

At the tip of Sandwich Harbour (Fig. 10A) the intensity of accretion varies greatly over time. The first northwards expansion of ca. 150m until 1994 followed an intense and short phase of erosion back to the initial sand spit dimension of 1984. From that on the sand spit was growing constantly until 2006. In total, it expanded 630m in northern direction with a mean annual accretion rate of 55m/a. After anew erosion in 2006 the sand spit expanded to its final dimension in 2014 with a total growth of 780m along the transect. The total change of 2280m (i.e. sum of erosion and accretion) along the transect is approx. three times higher (292%) than the total accretion of 780m. At Walvis Bay the total change is only 157% (660m) of the total erosion of 420m. This difference in total change reveals a more irregular and variable process at the tip of Sandwich Harbour compared to the overall steady erosion of the Walvis Bay's western flank (Fig. 10B).

279
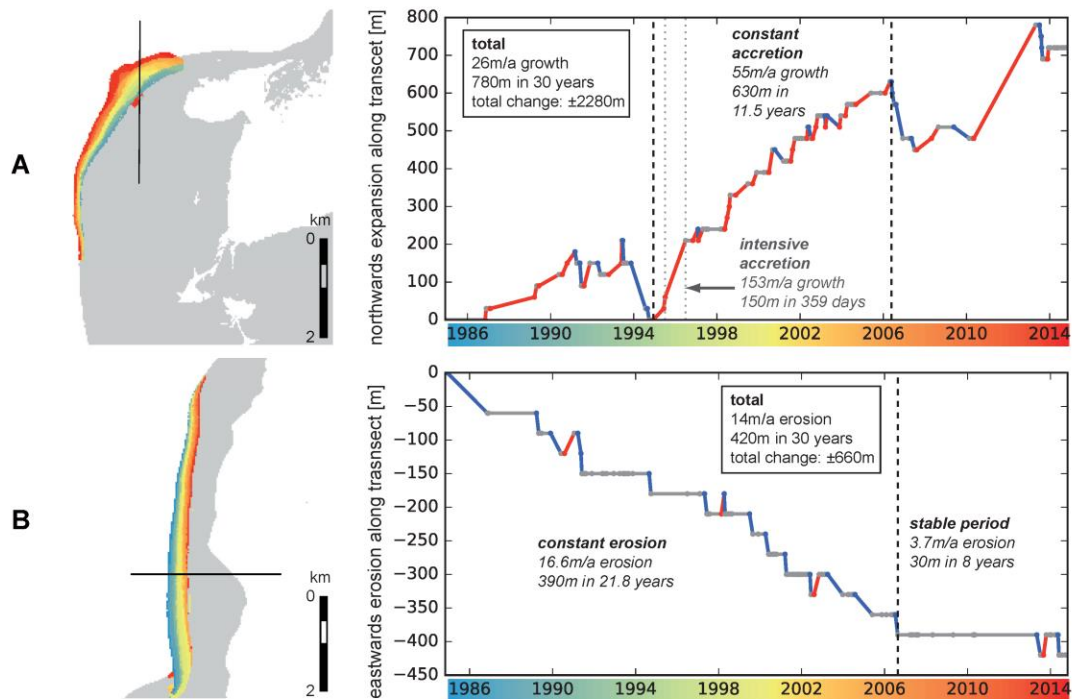
Figure 10 Detailed change along transects for the dominant accretion at the sand spit tip at Sandwich Harbour (A) and the dominant erosion of the sand spit's western flank at Walvis Bay (B). Left: Transect location depicted on the subsets of Fig. 8A1 and 9A1. Right: Change along the transect. Y-Axis: Change in meter with 1984 as starting point 0; dots represent datasets of the Landsat time series; connectors between dots represent the occurred change between these datasets (blue: erosion, red: accretion, grey: stable).

4.4 Validation

4.4.1 Qualitative Evaluation

The visual quality assessments of regions with dominating changes revealed that the WLMO approach detected the areas and the dates of changes correctly, which shows the robustness of the approach against temporary influencing factors such as clouds, fog, and small geometric shifts (see Supplements 1,2). In the highly variable tidal flats the approach occasionally has missed land/water transitions if the return period of sure water or sure land pixels was shorter than the median filter kernel of three temporal acquisitions (Fig. 5A) However, these rare misidentifications at the tidal flats have no influence for the evaluation of the spatiotemporal accretion and erosion processes at the sand spits of the coastal lagoons. According to Walvis Bay Salt Holdings (2017) and DMC and CSIR (2010) the approach has successfully identified the main expansions of the salt mining pre-evaporation ponds in 1988, 2000, and 2001 (Fig. 8).

The identification of the inland water ponds (Fig. 7), unknown to the authors before, proofed the objectivity of the approach to detect land/water transitions of any kind. The fact that almost no changes were identified at the stable coast of Walvis Bay and the stable eastern flanks of both sand spits (Fig. 7) confirms a very low susceptibility of the approach to identify false positives.

4.4.2 Influence of tides on the horizontal shoreline variations

For Walvis Bay basic bathymetry information can be found in DMC and CSIR (2010), Elfrink et al. (2003), Hughes et al. (1992), and Schoonees et al. (1998). The western flank, exposed to the open ocean, is much steeper than the eastern flank of the sand spit towards the protected lagoon and Walvis Bay city. For Donkey Bay (Fig. 1B), the most gentle part of the sand spits western flank (e.g. Elfrink et al., 2003, Fig. 1),

305 Schoones et al. (1998, Fig. 2) present an offshore slope of approximately 3.6°. At such a given slope of 3.6°
306 and 30m spatial resolution of a Landsat pixel, the tide range between two images needs to exceed 1.89m
307 to lead to an uncertainty in horizontal shoreline extraction of more than one Landsat pixel.

308 According to DMC and CSIR (2010) and Hughes et al. (1992) the tides at the two lagoons are semi-diurnal
309 with a mean tide range of 1.42m and 0.62m for spring tides and neap tides, respectively. Both, spring and
310 neap tides, fall below the 1 pixel uncertainty limit of 1.89m, meaning that the uncertainty of shoreline
311 extraction introduced by tide variations is within the sub-pixel range. Besides these two tide parameters
312 given in the literature, we analyzed the actual time series of tide data at Walvis Bay tide gauge. This gauge
313 is part of the Global Sea Level Observing System GLOSS (Caldwell et al., 2015) and tide data is available,
314 with some data gaps, since 1959 (UHSLC, 2018). Fig. 11 shows the tide height variations at Walvis Bay,
315 presenting a maximal tidal range (minimum and maximum of the whole time series) of approximately
316 2.1m and highest tide frequencies at 0.7m and 1.3m for low and high tides, respectively. Considering the
317 maximum tidal range of 2.1m by a given slope of 3.6° the horizontal uncertainty amounts to 33m,
318 representing an uncertainty of shoreline extractions of approx. one pixel if two subsequent Landsat images
319 would had been acquired at the two long-term tidal extremes. Ninety percent of all tide heights are within
320 a range of 1.3m (350mm-1630mm), resulting to 20m horizontal shoreline variations, which means subpixel
321 uncertainty in Landsat-based shoreline extraction. Overall, the horizontal uncertainty at Donkey Bay can
322 be expected to be less than one Landsat pixel.

323 Compared to Donkey Bay, the rest of the sand spits western flank at Walvis Bay is much steeper (e.g.
324 Elfrink et al., 2003, Fig. 1) and thus tide variations alter the horizontal shoreline position even less, which
325 means that tides can be neglected for the Landsat-based analysis in these regions. The fact that the more
326 gentle parts at the eastern flank (compared to Donkey Bay) are identified as stable (Figs. 6,7) shows further
327 the robustness of the WLMO approach, against tidal variations even if the horizontal shoreline
328 uncertainty might be higher than one pixel.
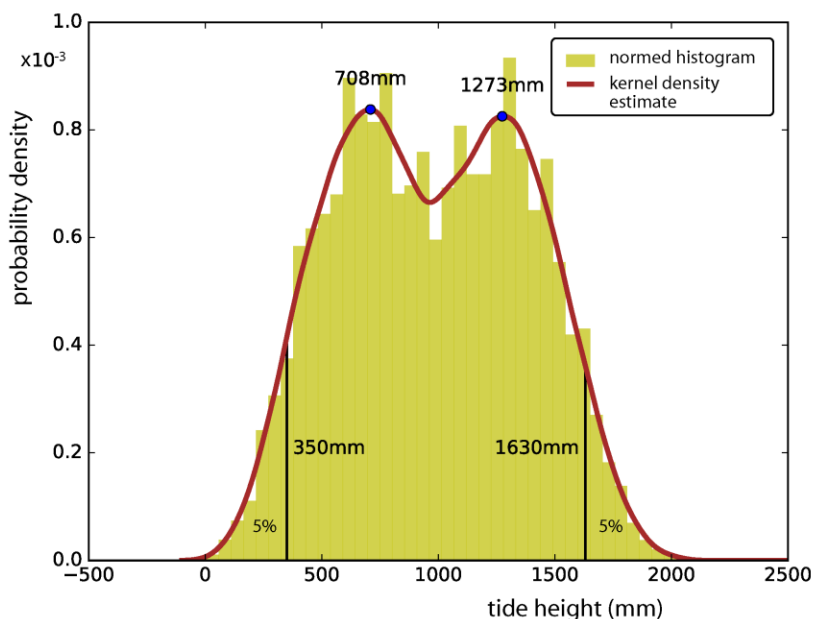
329

330 *Figure 11 – Tide height variation statistics at the Walvis Bay tide gauge since 1959.*

5 DISCUSSION

This paper proposed the WLMO (Water-Land-MOnitor), suited for the reconstruction of spatiotemporal shoreline variations by utilizing dense Landsat time series data. It focusses on the robust change assessment based on temporal MNDWI trajectories without the necessity to entirely map the shoreline position in each image. Thus, the in other studies (e.g. Ghosh et al., 2015; Kuleli, 2010; Louati et al., 2015; Wang et al., 2017) typically needed binarization of an image in water and non-water pixel for extracting the shoreline position is not strictly needed. Instead the WLMO includes a third class representing unsure pixels which are not sure water and sure land pixels. This allows the WLMO to detect changes only if the sure classes are changing and not in uncertain cases (such as wet surfaces, fog, and mixed pixels at the water-land front), in which other algorithms have to decide in each image if its water or not. That robustness of the change algorithm allows the integration of many images and to densify the analyzed data time series, making it possible to detect short-term changes in addition to the long-term change rates between several years or even decades that are typical periods in studies using optical satellite remote sensing data (e.g. Ghosh et al., 2015; Kuleli, 2010; Li and Damen, 2010; Wang et al., 2017). The implemented median filtering to despike the MNDWI-trajectory makes the WLMO also robust against outliers such as cloud coverage. However, by eliminating outliers it is always possible to eliminate real changes looking alike. In case of the WLMO it means that if accretion and erosion happen during three subsequent images the approach is not able to detect it. However, accretion processes are usually slow, which means that such a cycle (water<->land) does usually not happen in quick succession. Thus, using a dense time series minimizes the probability of missing such temporally variable accretion or erosion processes.

The results revealed that both sand spits at Walvis Bay and Sandwich Harbour expanded in northern direction along the shore. In the 30-year period between 1984 and 2014 the approach identified the maximum northern progression of the sand spit of 950 m (31.7m/a) at Walvis Bay and 1050m (35 m/a) at Sandwich Harbour. These northern longshore expansions correspond with the prevailing south and south-westerly wind, ocean current, and wave direction (see Section 2). This overall northern expansion for Sandwich Harbour has already been described in the literature (Wilkinson et al., 1989), nevertheless, it has never been quantified before. At Walvis Bay, Schoonees et al. (1998) and Hughes et al. (1992) determined an annual progression rate of 17m/a over the 20th century by examining nautical maps and aerial photographs. In comparison, our detected annual rate over the 30 year period of 1984-2014 of 31.7m/a is almost twice as high. Our finding correlates well with higher change rates for the more recent times, such as found by Ward (1989) and Schoonees et al. (1998), who reported expansion rates of 26m/a (1932 - 1989) and 22.6m/a (1980 - 1996), respectively. Another identified dominant change at Walvis Bay is the eastern directed erosion at the western flank, which decreased the width of the northern sand spit (Fig. 7). In Schoonees et al. (1998) this shrinkage was qualitatively discussed and the authors stressed the risk of potential sand spit breaching. In our study we were able for the first time to quantify this erosion with an annual rate of up to 14 m/a from 1984 to 2014 (Fig. 10B). The thinnest and thus probably the most vulnerable part for breaching could be identified in the middle of the northern sand spit, where its width has reduced from 750m to 360m with an rate of 13m/a (Fig. 7).

In contrast to previous studies at theses lagoons the developed WLMO approach derives not only long-term change rates but also spatially explicit change rates as well as their variations over time. For example, it could be shown that the ocean-exposed sand spit at Walvis Bay is characterized by areas of dominant

erosion and accretion, whereas in Sandwich Harbour dominant erosion is missing. This difference exists although both sand spits underlay mainly the same wind, wave, and ocean current processes (see Section 2). Thus, the absence of steady erosion at Sandwich Harbour might instead be explained by a higher sediment supply from the nearby Namib (Holdt and Eckardt, 2017) or by a different shaped shelf with less destructive wave energy at the shoreline. The argument of higher sediment supply is also supported by the four times larger sand spit accretion at Sandwich Harbour compared to Walvis Bay (1.71km² vs. 0.39km²). Moreover, this paper clearly demonstrated that the erosion and accretion processes at both lagoons greatly varied over time and thus cannot a priori be assumed as linear long-term processes. The tips of the sand spits for example underwent long-term longshore progradations but also short-term regressions (Fig. 8B3, 9B1, 10A) which are most likely caused by strong cross-shore wind and wave activity. In contrast to the longshore accretion the erosion at the western flank of Walvis Bay was a more constant process (Fig. 8B1, 10B), which implies no or negligible sediment transport in western direction.

The observed spatiotemporal sand spit dynamics also allow the evaluation of the risk of the lagoon's habitats to get destroyed. Overall, both sand spits have a stable eastern shoreline (Fig. 7) that shows that the lagoons are currently at a low risk to dry out because of silting. However, at Walvis Bay the ongoing erosion of the western flank increases the risk of future sand spit breaching, which has the potential to expose parts of the bay and the city to the open ocean. At Sandwich Harbour the frequent formation of sand barriers show the constant risk that the lagoon will be cut off from the open sea water, which could lead to a drying-out of the lagoon because of increased sedimentation. However, in the analyzed period these sandbanks were always eroded before they could connect the sand spit and the main coast, indicating a reduced risk after all.

6 CONCLUSION

This paper presents the WLMO (Water-Land MOnitor) approach for the mapping and monitoring of spatiotemporal changes of coastal shorelines using remote sensing time series data. It is based on pixel-oriented analysis of temporal MNDWI trajectories to distinguish efficiently between land and water and to determine the period of their temporal variations, i.e. accretion (water to land) and erosion (land to water). With four implemented steps, the temporal MNDWI-trajectory analysis is designed to accommodate the uncertainties that arise in common mono-temporal shoreline extraction techniques from the existence of clouds, turbidity, fog, tidal areas, wet surfaces, mixed pixels at the water-land front, and geometric mismatches between compared images.

Applied to the two Namibians coastal lagoons Walvis Bay and Sandwich Harbour, the approach revealed new qualitative and quantitative insights of the lagoon's spatiotemporal dynamics between 1984 and 2014 that go far beyond the long-term change rates that have been known before. It could be shown that long-term erosion and accretion of the lagoon's sand spits are non-linear processes that underwent great variations over time. Such variations were in detail demonstrated at the tips of the sand spits, which were characterized by overall longshore accretion that were occasionally interrupted by short-term regressions (erosion events) probably due to cross-shore wind and wave activity. The spatially explicit results of the approach also allowed a quantitative comparison of the occurred changes at the two coastal lagoons. At Sandwich Harbour the accretion at the sand spit was four times larger, indicating its higher supply of sediments from the nearby Namib Desert. Moreover, we were able to identify the main risks that threaten

the habitats of the coastal lagoons. At Walvis Bay the ongoing eastern directed erosion reduced the width of the sand spit significantly, and thus increased the risk of sand spit breaching which would expose a part of the lagoon and city to the open ocean. At Sandwich Harbour the main risk could be found in the frequent sand barrier formations at the mouth of the lagoon, which could result in the separation of the lagoon from the open ocean and thus to an increased sedimentation.

The approach builds solely on the use of the MNDWI for the differentiation between water and land, and could be directly transferred to other coastlines worldwide. This transfer might require adapting the threshold for sure land classification to different natural conditions, especially if coastal areas are vegetated and thus differ from the arid conditions of Namibian lagoons. Moreover, it can be extended to other multispectral sensors to condense the analyzed time series and thus shorten the intervals between which changes can be identified. Suitable data for such an extension would be the free of charge data of the sensor systems Sentinel-2 (Drusch et al., 2012) and ASTER both comprising the required spectral bands for the MNDWI used in this study.

REFERENCES

Aedla, R., Dwarakish, G.S., Reddy, D.V., 2015. Automatic Shoreline Detection and Change Detection Analysis of Netravati-Gurpur Rivermouth Using Histogram Equalization and Adaptive Thresholding Techniques. Aquat. Procedia, (ICWRCOE'15) 4, 563–570. https://doi.org/10.1016/j.aqpro.2015.02.073

Ahmed, M.H., El Leithy, B.M., Thompson, J.R., Flower, R.J., Ramdani, M., et al., 2009. Application of remote sensing to site characterisation and environmental change analysis of North African coastal lagoons. Hydrobiologia 622, 147–171. doi:10.1007/s10750-008-9682-8

Anthony, A., Atwood, J., August, P., Byron, C., Cobb, S., et al., 2009. Coastal Lagoons and Climate Change: Ecological and Social Ramifications in US Atlantic and Gulf Coast Ecosystems. Ecol. Soc. 14, 8.

Bates, P.D., Wilson, M.D., Horritt, M.S., Mason, D.C., Holden, N., Currie, A., 2006. Reach scale floodplain inundation dynamics observed using airborne synthetic aperture radar imagery: Data analysis and modelling. J. Hydrol. 328, 306–318. https://doi.org/10.1016/j.jhydrol.2005.12.028

Behling, R., Roessner, S., Segl, K., Kleinschmit, B., Kaufmann, H., 2014. Robust Automated Image Co-Registration of Optical Multi-Sensor Time Series Data: Database Generation for Multi-Temporal Landslide Detection. Remote Sens. 6, 2572–2600. doi:10.3390/rs6032572

Cermakova, I., Komarkova, J., Sedlak, P., 2016. Using Uav to Detect Shoreline Changes: Case Study - Pohranov Pond, Czech Republic, in: Halounova, L., Safar, V., Toth, C.K., Karas, J., Huadong, G., et al. (Eds.), Xxiii Isprs Congress, I. Copernicus Gesellschaft Mbh, Gottingen, pp. 803–808.

Coppin, P., Jonckheere, I., Nackaerts, K., Muys, B., Lambin, E., 2004. Digital change detection methods in ecosystem monitoring: a review. Int. J. Remote Sens. 25, 1565–1596. https://doi.org/10.1080/0143116031000101675

Costanza, R., D'Arge, R., De, G., Farber, S., Grasso, M., Hannon, B., Limburg, K., Naeem, S., O'Neill, R.V., Paruelo, J., Raskin, R.G., Sutton, P., Van, D.B., 1997. The value of the world's ecosystem services and natural capital. Nature 387, 253–260. https://doi.org/10.1038/387253a0

Caldwell, P. C., Merrifield, M. A., Thompson, P. R. 2015, Sea level measured by tide gauges from global oceans — the Joint Archive for Sea Level holdings (NCEI Accession 0019568), Version 5.5, NOAA National Centers for Environmental Information, Dataset, doi:10.7289/V5V40S7W.

458 DMC, CSIR, 2010. Environmental impact assessment Study for Strategic Expansion of the Walvis Bay
459   Container Terminal. Final Environmental Impact Report and Environmental Management Plan.
460   (No. CSIR/CAS/EMS/ER/2009/0029/A).
461 Drusch, M., Del Bello, U., Carlier, S., Colin, O., Fernandez, V., et al., 2012. Sentinel-2: ESA's Optical High-
462   Resolution Mission for GMES Operational Services. Remote Sens. Environ. 120, 25–36.
463   doi:10.1016/j.rse.2011.11.026
464 El-Asmar, H.M., Hereher, M.E., 2011. Change detection of the coastal zone east of the Nile Delta using
465   remote sensing. Environ. Earth Sci. 62, 769–777. doi:10.1007/s12665-010-0564-9
466 Elfrink, B., Prestedge, G., Rocha, C.B., Juhl, J., 2003. Shoreline evolution due to highly oblique incident
467   waves at Walvis Bay, Namibia. Coast. Sediments 3.
468 Ghosh, M.K., Kumar, L., Roy, C., 2015. Monitoring the coastline change of Hatiya Island in Bangladesh
469   using remote sensing techniques. Isprs J. Photogramm. Remote Sens. 101, 137–144.
470   doi:10.1016/j.isprsjprs.2014.12.009
471 Glassom, D., Branch, G., 1997. Impact of predation by greater flamingos Phoenicopterus ruber on the
472   macrofauna of two southern African lagoons. Mar. Ecol. Prog. Ser. 149, 1–12.
473   doi:10.3354/meps149001
474 Holdt, J.R. von, Eckardt, F.D., 2017. Dust activity and surface sediment characteristics of the dustiest river
475   in southern Africa: the Kuiseb River, Central Namib. South Afr. Geogr. J. 0, 1–18.
476   doi:10.1080/03736245.2017.1339627
477 Walvis Bay Salt Holdings, 2017. URL http://www.wbsalt.co.za/company/ (accessed 7.7.17).
478 Hughes, P., Brundrit, G.B., Searson, S., 1992. The Vulnerability of Walvis Bay to Rising Sea Levels. J. Coast.
479   Res. 8.
480 Kuleli, T., 2010. Quantitative analysis of shoreline changes at the Mediterranean Coast in Turkey. Environ.
481   Monit. Assess. 167, 387–397. doi:10.1007/s10661-009-1057-8
482 Lass, H.U., Mohrholz, V., 2005. On the fluctuations and vertical structure of the shelf circulation off Walvis
483   Bay, Namibia. Cont. Shelf Res. 25, 1473–1497. doi:10.1016/j.csr.2005.04.012
484 Lee, I.-C., 2016. Instantaneous Shoreline Mapping from Worldview-2 Satellite Images by Using Shadow
485   Analysis and Spectrum Matching Techniques. J. Mar. Sci. Technol.-Taiwan 24, 1204–1216.
486   https://doi.org/10.6119/JMST-016-1026-9
487 Li, X., Damen, M.C.J., 2010. Coastline change detection with satellite remote sensing for environmental
488   management of the Pearl River Estuary, China. J. Mar. Syst. 82, S54–S61.
489   doi:10.1016/j.jmarsys.2010.02.005
490 Long, N., Millescamps, B., Guillot, B., Pouget, F., Bertin, X., 2016. Monitoring the Topography of a Dynamic
491   Tidal Inlet Using UAV Imagery. Remote Sens. 8, 387. https://doi.org/10.3390/rs8050387
492 Louati, M., Saidi, H., Zargouni, F., 2015. Shoreline change assessment using remote sensing and GIS
493   techniques: a case study of the Medjerda delta coast, Tunisia. Arab. J. Geosci. 8, 4239–4255.
494   doi:10.1007/s12517-014-1472-1
495 Maiti, S., Bhattacharya, A.K., 2009. Shoreline change analysis and its application to prediction: A remote
496   sensing and statistics based approach. Mar. Geol. 257, 11–23. doi:10.1016/j.margeo.2008.10.006
497 Mann, T., Westphal, H., 2014. Assessing Long-Term Changes in the Beach Width of Reef Islands Based on
498   Temporally Fragmented Remote Sensing Data. Remote Sens. 6, 6961–6987.
499   https://doi.org/10.3390/rs6086961
500 Martínez, M.L., Intralawan, A., Vázquez, G., Pérez-Maqueo, O., Sutton, P., Landgrave, R., 2007. The coasts
501   of our world: Ecological, economic and social importance. Ecol. Econ., Ecological Economics of
502   Coastal Disasters 63, 254–272. https://doi.org/10.1016/j.ecolecon.2006.10.022
503 Miller, R.M., Becker, T., 2008. The Geology of Namibia: Upper palaeozoic to cenozoic. Ministry of Mines
504   and Energy Geological Survey of Namibia.
505 Natesan, U., Thulasiraman, N., Deepthi, K., Kathiravan, K., 2013. Shoreline change analysis of Vedaranyam
506   coast, Tamil Nadu, India. Environ. Monit. Assess. 185, 5099–5109. https://doi.org/10.1007/s10661-
507   012-2928-y
508 Ramsar, 2017. URL http://www.ramsar.org/ (accessed 7.7.17).
509 Roux, P.J., 1974. Drift sand reclamation of Walvis Bay, South West Africa. Int. J. Biometeorol. 18, 121–127.
510   doi:10.1007/BF01452232
511 Ryu, J.H., Won, J.S., Min, K.D., 2002. Waterline extraction from Landsat TM data in a tidal flat - A case
512   study in Gomso Bay, Korea. Remote Sens. Environ. 83, 442–456. doi:10.1016/S0034-4257(02)00059-
513   7
514 Schoonees, J.S., Lenhoff, L., Raw, A.J., 1998. Preventing natural breaching of the major sand spit protecting
515   the port of Walvis Bay. Coast. Eng. Proc. 1.

516   Stockdon, H.F., Sallenger, A.H., List, J.H., Holman, R.A., 2002. Estimation of shoreline position and change
517   using airborne topographic lidar data. J. Coast. Res. 18, 502–513.

518   UHSLC Legacy Data Portal [WWW Document], URL https://uhslc.soest.hawaii.edu/data/ (accessed
519   1.3.18)

520   Wang, X., Liu, Y., Ling, F., Liu, Y., Fang, F., 2017. Spatio-Temporal Change Detection of Ningbo Coastline
521   Using Landsat Time-Series Images during 1976–2015. ISPRS Int. J. Geo-Inf. 6, 68.
522   https://doi.org/10.3390/ijgi6030068

523   Ward, J.D., 1989. Comments on the geomorphology of Walvis Lagoon and environs. (No. 13/7/3/1/3).
524   Geological Survey of South West Africa/Namibia, Windhoek.

525   Wilkinson, M.J., Blaha, J.E., Noli, D., 1989. A new lagoon on the Namibian coast of South Africa: Sand spit
526   growth documented from STS-29 shuttle photography. Geocarto Int. 4, 63–66.
527   doi:10.1080/10106048909354235

528   Xu, H., 2006. Modification of normalised difference water index (NDWI) to enhance open water features
529   in remotely sensed imagery. Int. J. Remote Sens. 27, 3025–3033. doi:10.1080/01431160600589179